ORIGINAL ARTICLE

Alginates as Green Flocculants for Metal Oxide Nanoparticles

Vladislav Slabov[1] · Garima Jain[2] · Irina Chernyshova[1] ·
Hanumantha Rao Kota[1] · Helga Ertesvåg[2]

© The Author(s) 2023

Abstract Flocculation is used for the removal or separation of colloids, e.g. in water treatment and mineral processing. Alginates are linear, anionic biopolymers composed of mannuronic (M) and guluronic (G) acids. The relative amount and distribution of M and G impact the ion-binding and gel-forming properties of the polymer, but still no one has yet addressed the impact of alginate composition on flocculation of nanoparticles or mineral particles. Our results showed that the distribution of G was important for flocculation, especially when Ca^{2+} was used as activating ion. With Ce^{3+} as activating ion, the shape and size of flocs were affected by alginate acetylation. This work expands the knowledge about the flocculation behavior of alginates and demonstrates that both bacteria- and algae-derived alginates can be potential biodegradable flocculants of ultrafine particles for mineral processing industry.

Keywords Nanoparticle flocculation · Alginate · Green flocculant · Iron oxide · Cerium oxide

Published online: 11 May 2023

1 Introduction

The removal or separation of nanoparticles (NPs) and sub-micron particles dispersed in aqueous media is generally challenging due to the associated disadvantages of the commonly used membrane filtration method [1]. In wastewater treatment and mineral processing, a common method to address this challenge is flocculation, which is used to separate colloids by their sedimentation as large aggregates (flocs). Polymers can assist in forming flocs from destabilized dispersion by acting as flocculants [2].

Polyacrylamide (PAM)-based polymers are the largest category of flocculants in mineral processing [3]. However, acrylamide monomers are toxic [4], but has been found to be one of the main degradation component of cationic PAM [5]. These polymers then need to be replaced by eco-friendly alternatives, for instance bio-based polysaccharides including starch, chitosan, fucoidan and alginate. Several studies have suggested their possible application in mineral processing and wastewater treatment [3, 6–9]. For starch, it has been shown that the linear form is more efficient for flocculation than the branched form, emphasizing the need for using well-characterized polymers when conducting such studies [10].

Alginates are 1–4 linked linear copolymers composed of mannuronic acid (M) and its C5-epimer guluronic acid (G) [11]. The polymer has many uses within industry, pharma and food [12, 13], the current market volume is 44.480 tons (2021) [14]. The isoelectric point of alginates is around 3.4–3.7 [15], which provides soluble, fully anionic polymers at pH above 4. The distribution of M and G vary between different alginate molecules depending on their source. Hence, alginate chains are described as composed of three block types; G-blocks contain consecutive G residues, M-blocks contain consecutive M residues, and MG-blocks
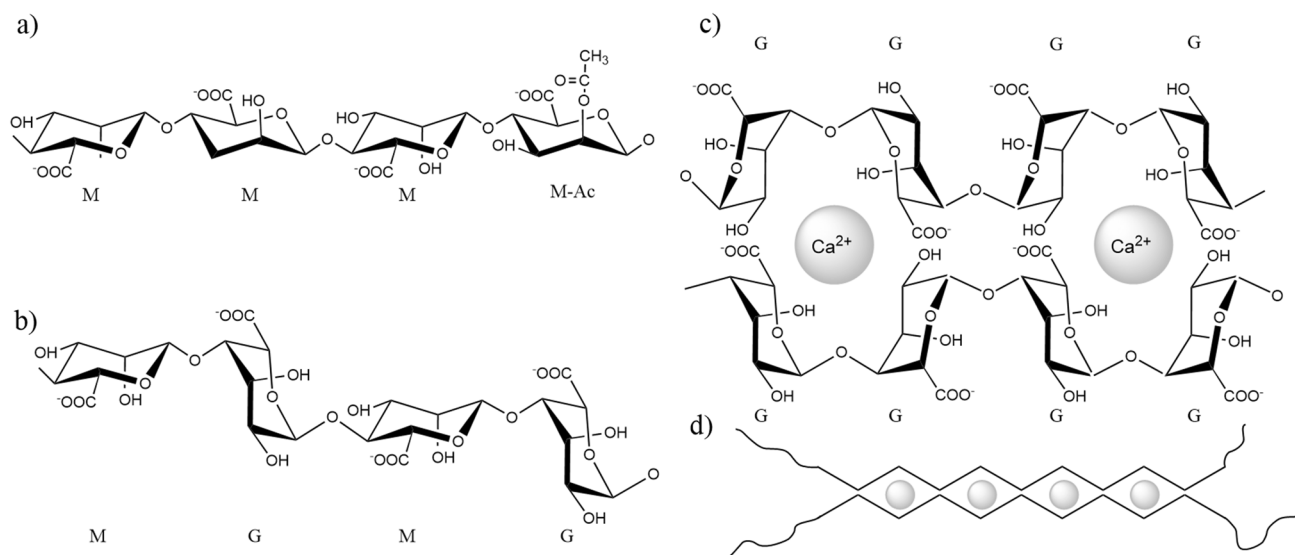
contain alternating M and G residues (Fig. 1). The number of residues in any block may vary from two to the length of the chain. The average structure of alginate samples is determined by combining ^{1}H-NMR analyses, HPAED-PAD, SEC–MALLS and specific lyases [13].

Commercial alginates are manufactured from brown algae, but alginates are also produced by bacteria from the genera *Azotobacter* and *Pseudomonas*. During biosynthesis, the organisms produce mannuronan, and some of the M-residues are then epimerized to G-residues by mannuronan C-5 epimerases acting on the polymer [11, 16]. Bacterial alginates can also be O-2 or O-3-acetylated [17]. There is a large variation between alginates produced by different species or even under different environmental conditions [11, 18]. Given that the two epimers have different structures in the polymer (Fig. 1), their relative amounts and distribution within the polymer affect the structure of the alginate and its ability to form gels as recently reviewed [15].

Alginates containing G-blocks form gels with divalent metal ions [15], where Ca-gels have been most studied. In the junction zones, two G-blocks are crosslinked by Ca^{2+}-ions coordinated by two adjacent G-residues on both chains (Fig. 1). The crosslinking then proceeds, the length of the junction zones is important for the gel strength [19]. It has been found that crosslinking with MG-blocks might extend these gel junctions [15]. G-blocks will also bind other alkaline-earth metal ions, the binding strength increases with the radius [20]. Other metal ions with higher valencies also bind alginates, however, for most of these, alginate composition does not influence binding [21, 22]. The coordination of individual ions depends on their size and valency [23–25],

however, how trivalent ions bind and crosslink the different block-structures are still not known [22].

The flocculation properties of alginates have been studied for a long time however, mostly algae-derived alginates have been used [8, 26–29] and it has been proposed that the formation of an alginate ionic gel network is needed for flocculation of the dispersed particles [29]. The previous research utilized native or modified alginates and various mono-, di- and trivalent salts [8, 28–32]. Still, most of these studies have not addressed the effect of the alginate composition on flocculation of dispersed particles, although it has been shown that it is important in water treatment [33].

Besides flocculant, alginates can be used as modifiers and depressants in mineral flotation, and as a sorbent for heavy metal removal. In particular, in scheelite flotation, alginate selectively depress calcite and fluorite [32]. In reverse flotation, alginate can support removal of quartz and chlorite from hematite ore [34]. Furthermore, alginate composites and alginate hydrogels effectively adsorb heavy metals (Se(IV), Cr(VI), As(V)) from wastewater [22, 35]. Hence, the interaction of alginates with colloidal mineral particles and multi-valence metal cations has a broad scope.

This work compares the flocculation properties of three well-characterized alginates with different G-content, G-distribution and acetylation, where our main motivation is to explore the effect of alginate composition on their ability to flocculate CeO_2 and α-Fe_2O_3 (hematite) NPs. These NPs serve as model systems for cerium, which is an abundant rare earth element and for iron, which is the most used metal. Since the flocculation performance of alginates depends on the cross-binding cation, we compare the efficiency of

divalent Ca^{2+} and trivalent Ce^{3+} on this process. The ionic radius of Ce^{3+} and Ca^{2+} is 0.102 nm and 0.100 nm, respectively [36], making them good candidates to study the effect of charge on the interaction between metal ions and alginates. We found that trivalent Ce^{3+} activates flocculation properties of alginate independently of its G-block content, while activation by Ca^{2+} requires G-blocks.

2 Material and Methods

2.1 Alginates

Protanal LF 10/60 TM sodium alginate (50% G-blocks, 17% MG-blocks and 33% M-blocks) from *Laminaria hyperborea* was obtained from FMC Biopolymer. Bacterial alginate was isolated from *Pseudomonas fluorescens* Pf201 (no G-blocks, 30% MG blocks, 70% M-blocks, degree of acetylation 0.4), the third was made by deacetylating this alginate [37] [17]. These alginates are specified as LF10/60, PfAc, and PfdeAc, respectively.

2.2 Chemicals

MilliQ water was used in all experiments. NaOH and HCl were used for pH adjustments and $NaNO_3$ as background electrolyte solution (all from VWR). $CaCl_2$ and $Ce(NO_3)_3 \cdot 6 H_2O$ (Merck) (prepared as 18 mM stock solutions) were used as metal cations for flocculation activation.

2.3 NPs

Cerium (IV) oxide (99.9%) 10 nm size was purchased from Meliorum Technology Inc. Hematite (α-Fe(III) oxide) (98%) 30–50 nm (Alfa Aesar 47,044) was purchased from Thermo Fisher Scientific. The initial concentration of CeO_2 and α-Fe_2O_3 NP dispersions in water was 200 and 300 mg/L, respectively. The stability of NPs dispersed in aqua solution is usually explained by a high ζ-potential, which should be >30 mV, but recent work with Fe_3O_4 NPs argues that this is not always the case [38, 39]. In our work we employed two days of ultrasonication to break possible aggregates of CeO_2 and α-Fe_2O_3 NPs [40]. These concentrations were then diluted to 50 and 75 mg/L for CeO_2 and α-Fe_2O_3, respectively, with pH around 5. After four weeks, no sedimentation was observed.

2.4 ζ-potential

The zeta (ζ) potential of NPs in water, alginate solutions or treated with Ca^{2+} and Ce^{3+} was measured using a Malvern ZetaSizer Nano Z (laser Doppler micro-electrophoresis) instrument. NPs were first dispersed in a 0.001 M $NaNO_3$ background solution at 0.1 wt. % by sonication for 20 min. This dispersion was split to prepare dispersions with the three alginate samples and one blank (in 0.001 M $NaNO_3$). Then, the prepared samples were split into 30-mL samples followed by pH adjustment of each sample and equilibration on a shaking table for 5 h. Afterwards, pH was readjusted with 0.01 M NaOH or HCl solutions before measuring its ζ-potential. As material settings in the ZetaSizer, we used refractive indices of 3.0 and 2.2 and absorption of 0.8 and 0.5 for iron and cerium oxide NPs, respectively.

2.5 Flocculation

To observe the flocculation process visually, experiments were conducted in glass vials in the presence and absence of alginate samples. Alginate stock solutions were prepared by dissolving alginates in MilliQ at 400 mg/L. All stock solutions were adjusted to pH 6–7. For the experiments, NPs dispersions with pH 6–7 were split into 10 mL samples and metal cations (Ca^{2+} or Ce^{3+}) were added to each dispersion to a concentration of 3 mM (after addition of alginates). The final concentrations of NPs were 44 mg/L for CeO_2 and 66 mg/L for α-Fe_2O_3. After shaking by hand, alginate stock solutions were slowly added to a final concentration of 50 mg/L over a period of one minute. The dispersions treated with alginate were shaken simultaneously for 5–10 s and then left still for further observation.

2.6 Kinetic Measurement of Flocculation

NP dispersions (10 ml) were conditioned with solutions of either Ca^{2+} or Ce^{3+} for one minute before adding alginates. Final concentrations were as above. The samples were vortexed for 10 s immediately after addition of alginates, moved to cuvettes and the optical density (OD) was recorded at 350 and 450 nm for iron oxide and cerium oxide NPs, respectively. These values were found by preliminary experiments to give good absorbance by the respective NPs. No mixing took place while the cuvette was standing in the spectrophotometer.

2.7 High Speed Camera Analysis of Flocculation

To estimate the shape and size of flocs, a high-speed camera (Chronos 1.4, Kron Technologies Inc.) mounted on an optical microscope (NIKON SMZ45T Stereoscopic Microscope) was used (Supplementary Figure S1). Ten ml NP dispersion pretreated by metal cations was placed into a Petri dish placed on a magnetic stirring (400 rpm), and alginate (50 ppm, ppm is defined as mg/L) was added. After one minute stirring was stopped and video recorded (10 s long, resolution 1280 × 1024, 1069 frames per second).

2.8 Transmission Electron Microscopy

The NPs were sonicated for 30 min in ethanol to obtain very dilute dispersion, which was drop-cast onto TEM copper grid and dried. TEM images were acquired using a JEOL 2100F electron microscope operated at 200 kV.

2.9 The Brunauer, Emmett, and Teller (BET) Specific Surface Area and Particle Size Distribution

The BET surface areas of NPs were measured using a Micromeritics Tristar 3000 Analyzer. The samples were degassed at 250 °C under helium flow for 3 h. Average values of two duplicate measurements are presented.

3 Results

3.1 *The Morphology of α-Fe$_2$O$_3$ and CeO$_2$ NPs*

One can see from the TEM images (Fig. 2) that α-Fe$_2$O$_3$ NPs have a needle-like shape, while CeO$_2$ NPs have a random, almost cubic shape. The electron diffraction patterns of α-Fe$_2$O$_3$ and CeO$_2$ confirm that the NPs are randomly oriented.

The BET surface area of CeO$_2$ NPs was found to be 72 ± 2 m^2/g, which was two times higher as compared to that of α-Fe$_2$O$_3$, having an area of 36 ± 1 m^2/g. This difference can be explained by the difference in the NP size.

3.2 ζ-potential of Iron and Cerium Oxide NPs in the Presence and Absence of Alginate

The ζ-potential of α-Fe$_2$O$_3$ and CeO$_2$ NPs (Fig. 3a, b) shows that the isoelectric point (IEP) of both NPs was around pH 7. This value is close to the values of 7.8 and 8 previously reported for hematite [41] and cerium oxide [42] NPs.

As expected, the anionic alginates PfAc, PfdeAc and LF 10/60 make the ζ-potential of the NPs negative (Fig. 3a,

b). The decreased charge was observed to be in the pH range from 3 to 10, meaning that at 30 ppm the polymer adsorbs to the NPs even when the ζ-potential of the NPs is negative. Furthermore, the value of ζ-potential became more negative than -30 mV, which could be categorized as a stable colloidal dispersion [43]. As a result, none of the three alginates initiated visible flocculation of NPs (Fig. 4).

3.3 ζ-potential of Iron and Cerium Oxide NPs in the Presence and Absence of Metal Cations

Since we wanted to use Ca^{2+} and Ce^{3+} as flocculation activators, we studied their effect on ζ-potential of the NPs in absence of alginates. Both metal ions should be presented in cationic form in the solution, according to a speciation diagram (Supplementary Figure S2). The result of the ζ-potential measurements (Fig. 3c, d) shows a strong shift of the NPs' IEP indicating adsorption of Ca^{2+} and Ce^{3+} on both NPs. As expected, in the presence of metal cations the ζ-potentials of the NPs increased for all measured pH values and became positive. The increase was significantly higher in the basic pH region when Ce^{3+} ion was added as compared to Ca^{2+}. A positive charge on NPs should enhance their binding with the anionic alginates.

3.4 Flocculation of Cation-Activated NPs

Firstly, the flocculation of NPs activated by cations was tested in glass vials. Dispersed iron oxide or cerium oxide NPs were mixed with Ca^{2+} or Ce^{3+} and then different alginates samples were added. The final concentrations were around 3 mM metal ions and around 50 ppm alginates, while pH was in the range of 6–7.

As was noticed before, the iron oxide NPs did not flocculate in the absence of the cations (Fig. 5a). In the presence of Ca^{2+}, visible flocs were observed only for the LF 10/60
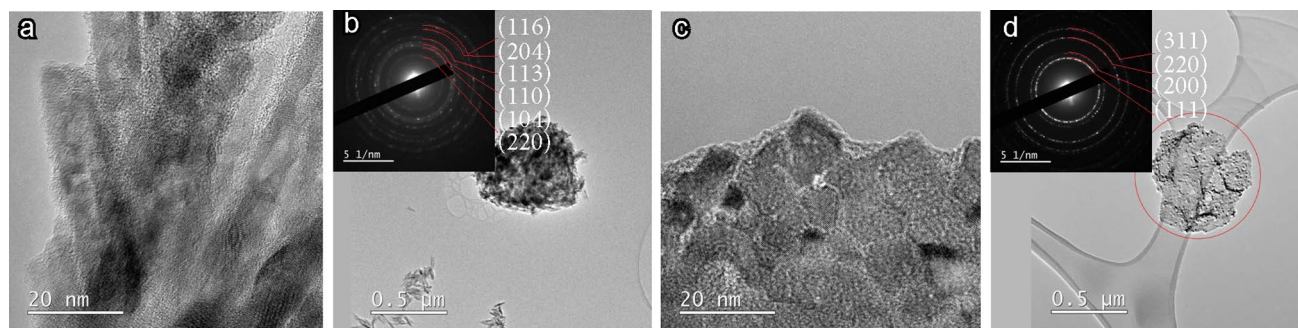

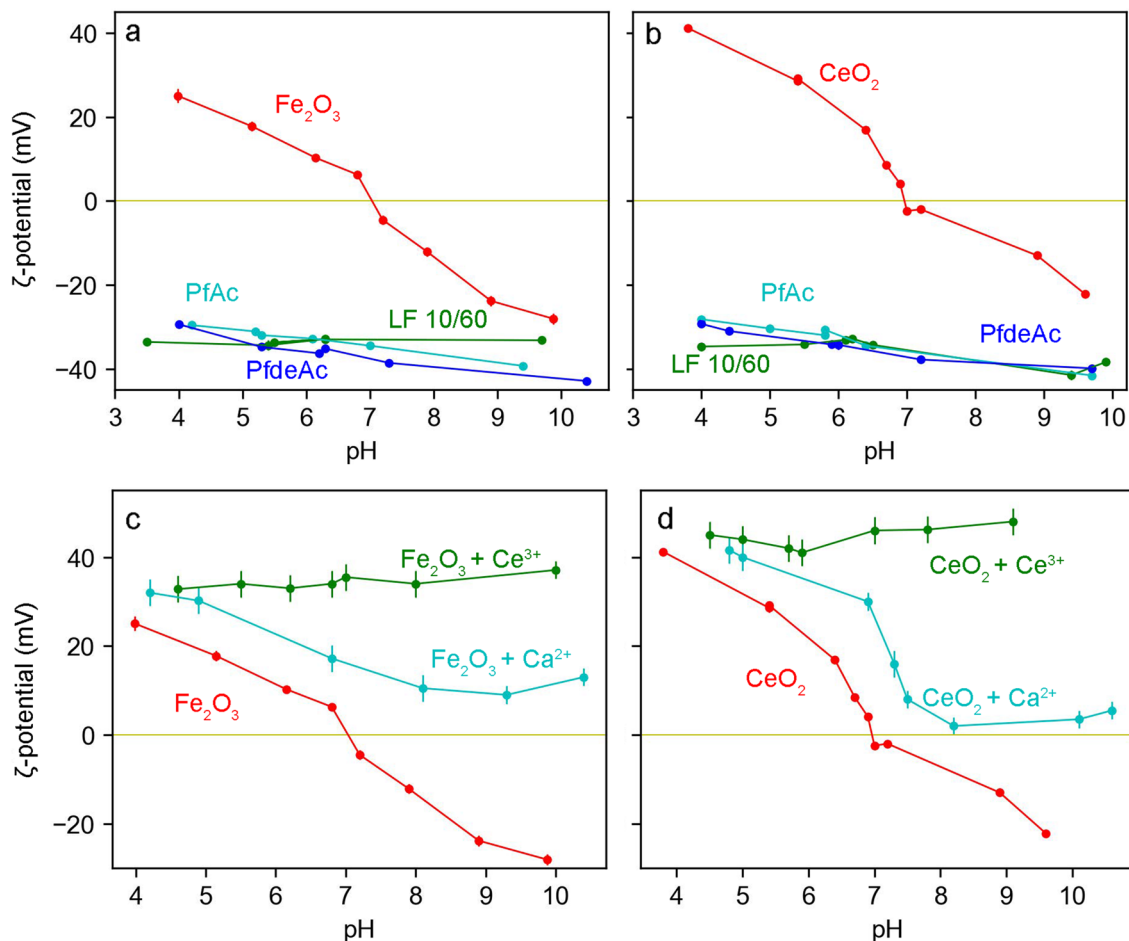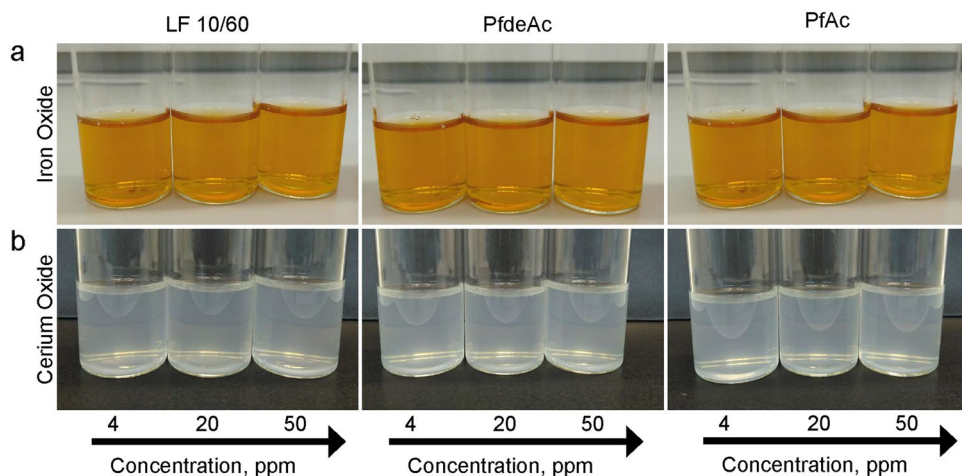**Fig. 2** TEM images of **a**, **b** α-Fe$_2$O$_3$ and **c**, **d** CeO$_2$ NPs

Fig. 3 pH dependence of the ζ-potential of **a** α-Fe₂O₃ and **b** CeO₂ NPs in the absence and presence of 30 ppm concentration of PfAc, PfdeAc and LF 10/60. **c** α-Fe₂O₃ and **d** CeO₂ NPs in the presence and absence of Ca²⁺ and Ce³⁺

Fig. 4 The effect of 4, 20 and 50 ppm concentrations of Lf 10/60, PfdeAc and PfAc on **a** α-Fe₂O₃ and **b** CeO₂ NPs dispersions at pH 6–7

alginate, while the dispersions treated by PfdeAc and PfAc showed no flocculation even after several hours. The same result was obtained for cerium oxide NPs (Fig. 5b). However, when activated by Ce³⁺ any combination of NP and alginate immediately flocculated (Fig. 5).

3.5 Evaluation of Flocculation by Time-Scale Experiments

While the above experiments showed that flocculation took place, changes in optical density (OD) over time were used
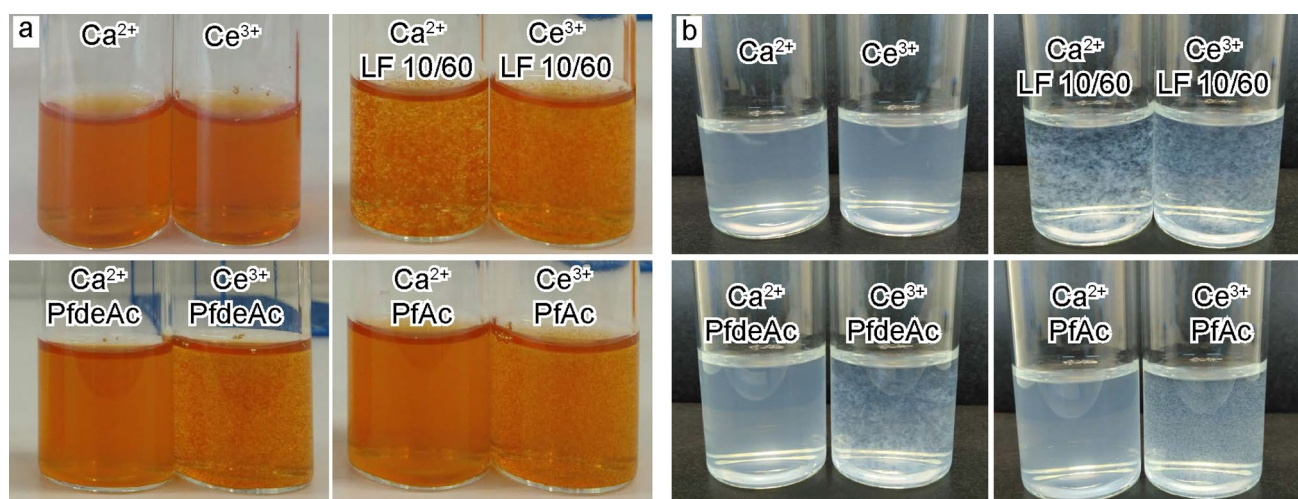
Fig. 5 The effect of 50 ppm of alginates on flocculation of **a** α-Fe$_2$O$_3$ and **b** CeO$_2$ NPs activated by 3 mM Ca^{2+} or 3 mM Ce^{3+}
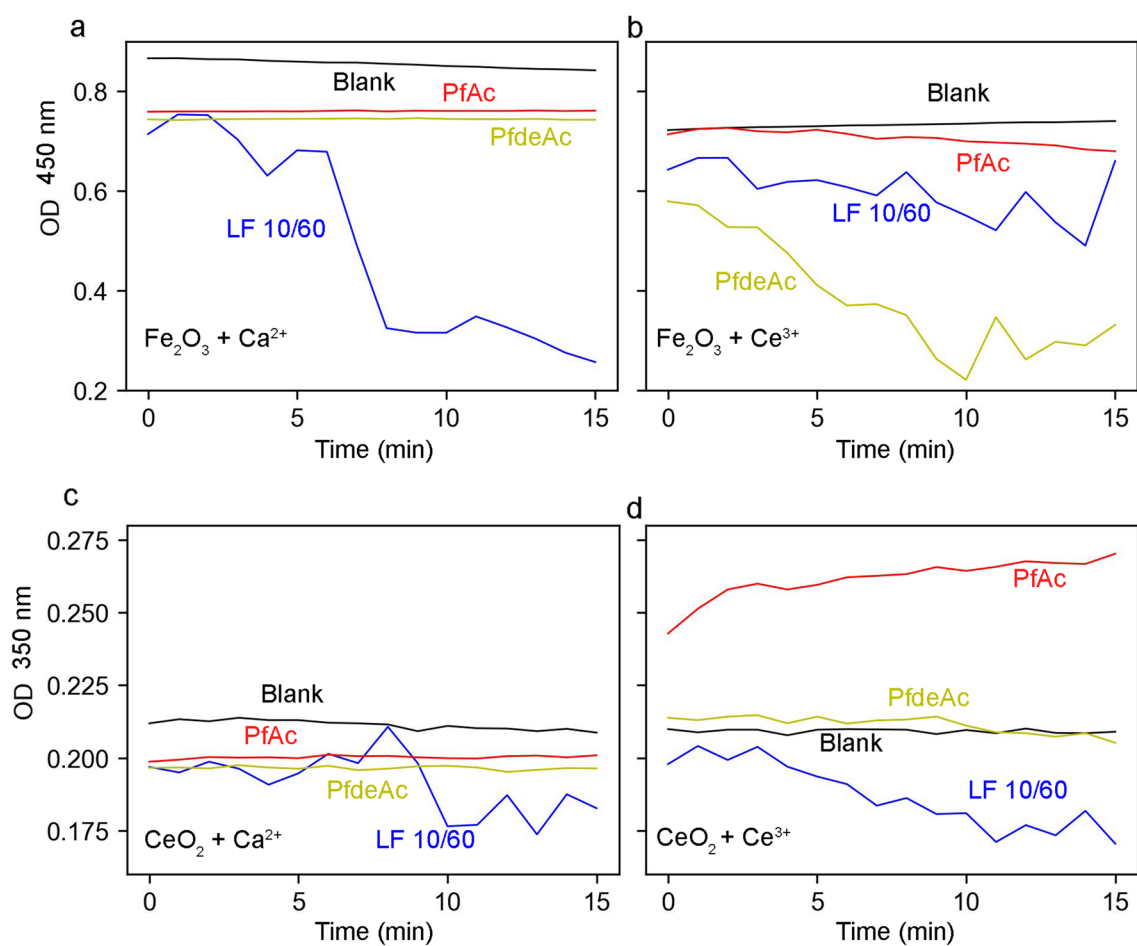

Fig. 6 The influence of NPs flocculation time on the optical density of the dispersions. The final concentrations of metal cations and alginate were 2.4 mM and 43 ppm, respectively. Blank samples contain NP and metal ion but no alginate

to compare the flocculation efficiency of alginates (Fig. 6). The decrease in OD should correlate with the removal of NPs, i.e. sedimentation of flocs. When only metal ions were added to the dispersions, there was a slight shift in initial OD, but no decrease with time (Supplementary Figure S3). These dispersions were used as blank samples in Fig. 6.

The strongest effect on flocculation of iron and cerium oxide NPs activated by Ca^{2+} was observed for the mixture with LF10/60 where the OD decreased from about 0.85 down to 0.3, and from around 0.21 down to around 0.18 for iron and cerium oxide, respectively (Fig. 6 a, c). In contrast, the NPs activated by Ca^{2+} did not flocculate when PfAc and PfdeAc were added; the OD of these systems slightly decreased and remained constant for 15 min (Fig. 6 a, c). These results confirmed the results from the initial flocculation experiments (Fig. 5).

As was expected from the initial experiments, Ce^{3+} affected the OD of the samples more than Ca^{2+}. PfdeAc showed the strongest effect of the three alginates on OD iron oxide NPs activated by Ce^{3+} (Fig. 6b). In contrast, PfAc had the weakest influence on the OD of cerium oxide NPs. When cerium oxide NPs were combined with Ce^{3+} cations, only LF10/60 were able to result in fast sedimentation of flocs (Fig. 6d). The final effect of LF10/60 on cerium oxide OD was similar for systems with Ca^{2+} and Ce^{3+}. However, the shapes of the curves were very different, which could indicate a difference of the formed flocs (Fig. 6c, d).

3.6 Evaluation of the Effect of Alginate Concentration on Flocculation

To study the concentration effect of the alginates on NPs flocculation, we conducted time-scale experiments for LF 10/60 and PfdeAc at concentrations 5, 15, 30, 44 and 90 ppm. The systems of iron oxide NPs activated by Ca^{2+} and Ce^{3+} were chosen due to the strongest flocculation effect from the previous tests. Figure 7 shows the result of OD changes over 10 min for alginates at different concentrations of alginates. As observed earlier (Fig. 6), the initial OD measurements was influenced by the addition of alginates. Moreover, this effect appears to be dose dependent with an intermediate dose giving the lowest initial OD value. The flocculation seems to start immediately after mixing, since we see a dosage dependent change in OD after only one minute for both LF10/60 (Fig. 7a) and PfdeAc (Fig. 7b).

We observed flocs for all tested concentration of LF 10/60. The flocs at 5 ppm concentration were smaller than the others, and this could have prevented their sedimentation in this experiment. The flocs formed at 15 and 30 ppm were also visibly denser than those formed at the highest alginate concentrations, and sedimented faster (Fig. 7a). According to this, the concentration of 15 ppm of LF 10/60 is the most favorable for the rapid sedimentation of flocs. However, at 10 min the OD is not significantly different for the concentrations in the range of 15–44 ppm, and the observed results could be a result of the short mixing time, the higher concentrations might need more time to reach equilibrium.

For each concentration of PfdeAc in the presence of Ce^{3+}, except 5 ppm, we observed flocs. At 5 ppm, the OD did not change during the 10 min. (Fig. 7b). From Fig. 7b one can see that PfdeAc dosages of 30 and 44 ppm are the most effective ones.

The sedimentation of iron oxide flocs was also tested for the Lf10/60-Ca^{2+} and PfdeAc-Ce^{3+} systems in glass vials, using 44 ppm alginate concentration and 1.5 min mixing time (Fig. 8). Flocs had formed in both systems when the
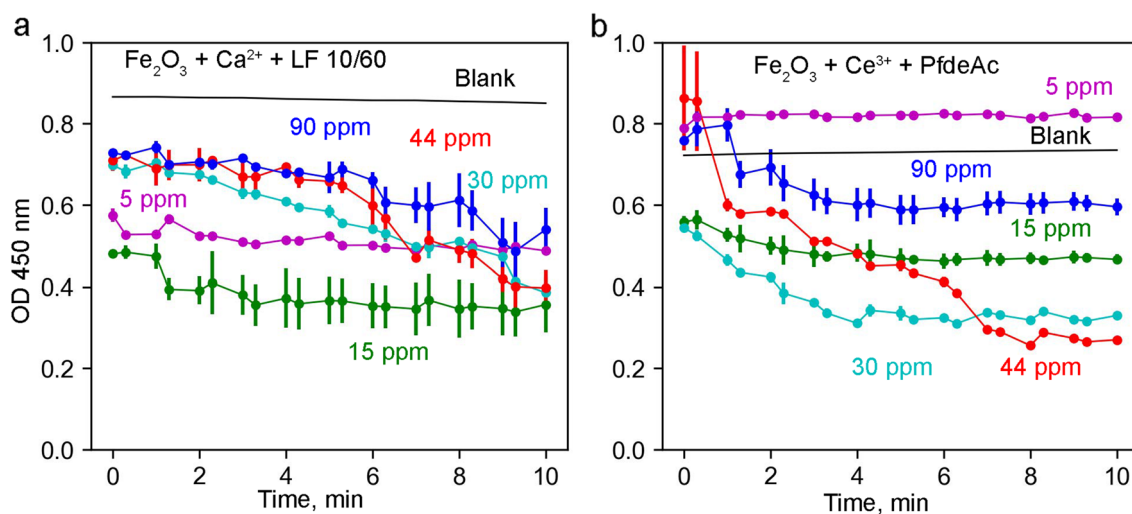

Fig. 7 The flocculation dependence of iron oxide NPs on alginate concentration: **a** LF 10/60 and **b** PfdeAc activated by Ca^{2+} and Ce^{3+}, respectively. Blank samples contain NP and metal ion but no alginate
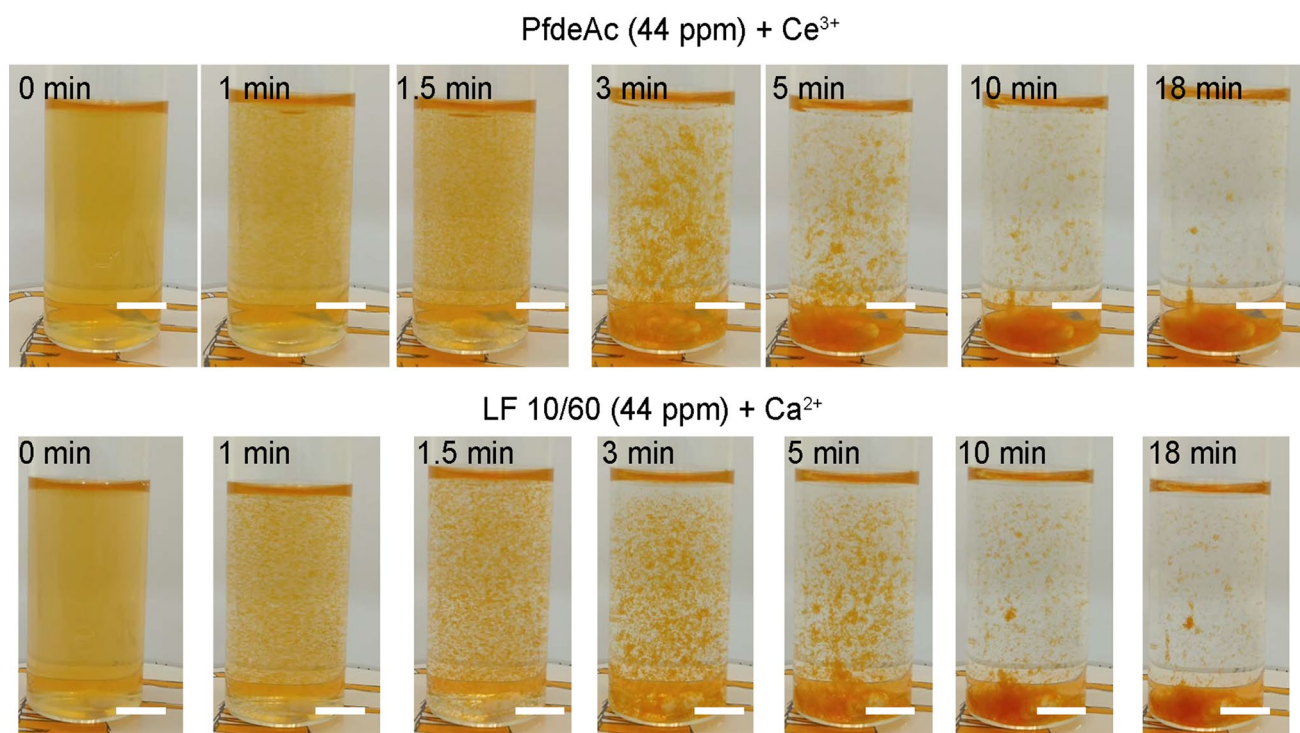
Fig. 8 Sedimentation of α-Fe$_2$O$_3$ flocs generated by PfdeAc-Ce^{3+} (*top*) and Lf10/60-Ca^{2+} (*bottom*) alginates. The alginates were added at t = 0 min to NPs dispersions containing 3 mM metal cations that were being stirred at 400 rpm. Stirring was halted at t = 1.5 min, and sedimentation was observed thereafter. Scale bar 1 cm

stirring were stopped, and already after 10 min most of the particles had settled on the bottom, confirming the results obtained from the spectroscopy experiment.

3.7 Floc Shape Depends on Alginate Type and NPs Size

The differences in sedimentation could potentially be caused by differences in the shape or size of flocs. To compare flocs shape, we used a high-speed camera mounted on an optical microscope. The studied NP dispersions in the Petri dish were placed on the magnetic stirrer, and then first the cations and then alginate samples were added. After an interaction time of one minute, stirring was stopped and images were obtained for further analysis (Fig. 9).

The shapes of the iron oxide flocs differed depending on the alginate. The flocs were similar in the LF 10/60 systems activated by Ca^{2+} and Ce^{3+}. However, flocculation of NPs by PfAc and PfdeAc differed according to their shape and size. Thus, iron oxide activated by Ce^{3+} increased in size in the followed sequence of alginate samples: Lf10/60 ≤ PfAc < PfdeAc. These flocs resembled flat flakes and seemed similar in shape. Big flocs should sediment faster, and we can observe the expected stronger effect on OD of PfdeAc (Fig. 7b).

The pale white flocs were less visible than the reddish flocs containing iron NPs, making it harder to compare their size and shape (Fig. 9). As observed for iron oxide NPs, flocs of cerium oxide NPs formed by LF 10/60 and activated by either Ca^{2+} or Ce^{3+} were similar. We can clearly see the formation of fiber-like flocs by PfdeAc, while PfAc forms flocs like those formed by LF 10/60, showing that both G-blocks and acetylation affects the size and shape of cerium oxide NPs flocs. During the experiment, web-like structure was observed in the dispersion, and these did not sediment fast. This could explain the observed weak decrease in OD for the corresponding sample in the OD study (Fig. 6d, PfdeAc).

4 Discussion

Following production and usage of nanomaterials, their migration in waters, soil and atmosphere causes increased environmental issues [44, 45]. Each year the worldwide production of nanomaterials counts tens and hundreds of tons. Specifically, based on 10 years old data, the median worldwide productions of FeO$_x$ and CeO$_x$ is 55 t/year [46]. Moreover, mining and mineral processing generate waste containing NPs, which are difficult to reprocess [47, 48]. Flocculation can be a solution for wastewater treatment or used to reduce the amount of waste in mineral processing industries. Expanding the knowledge of flocculation agents
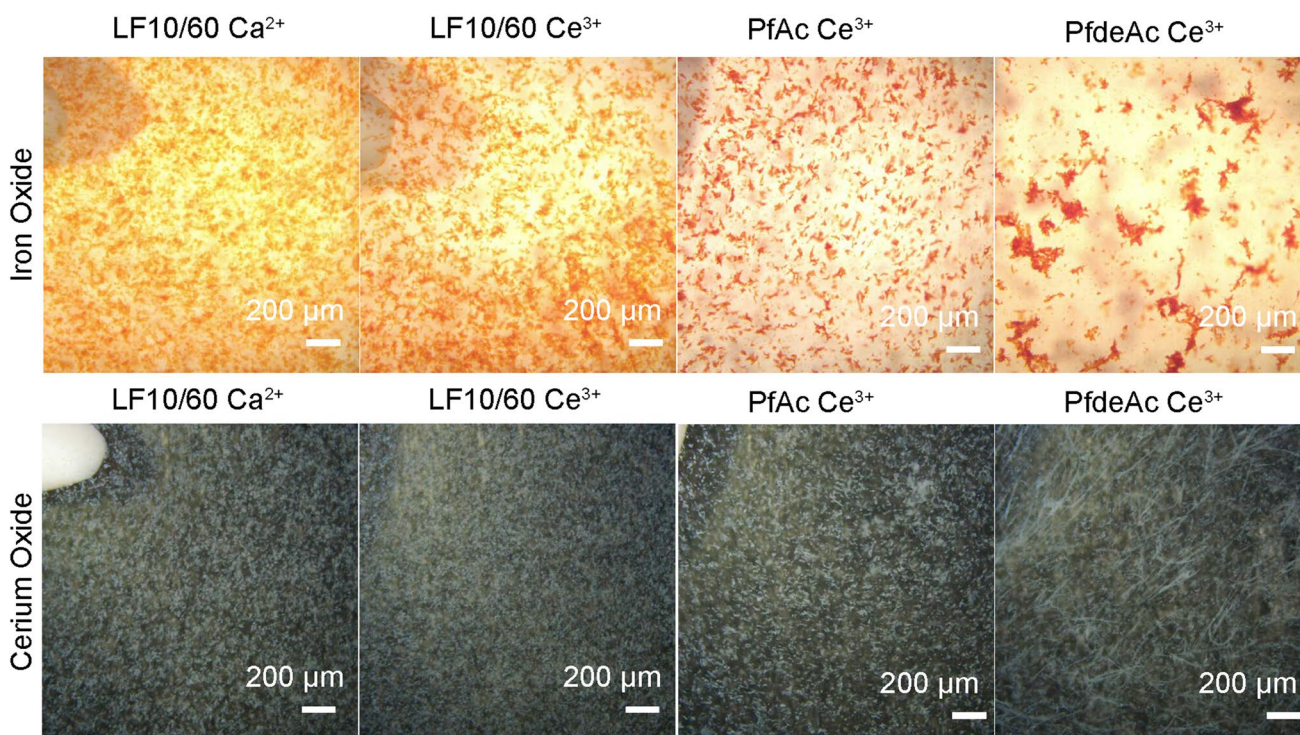
Fig. 9 High speed camera images of flocks taken after 1 min of stirring at 400 rpm. Iron oxide (*top*) and cerium oxide (*bottom*) NPs activated by Ca^{2+} or Ce^{3+}, and flocculated by LF 10/60, PfAc or PfdeAc

will help to reach maximum efficiency in the dewatering processes and find the most sustainable products.

The flocculation process by polymers requires bridging between dispersed particles or their charge neutralization [43]. For bridging to happen, only parts of the polymer should be adsorbed on one particle surface, leaving at least enough polymer length to form a bridge and adsorb to a second particle (Fig. 10a). The ζ-potential results demonstrate adsorption of all studied alginate samples since their IEP is shifted from initial pH (Fig. 3a, b). However, alginate adsorption did not cause any flocculation, in contrast, ζ-potential results show stabilization of NPs dispersions from acidic to basic pH [49, 50]. This is most easily

Fig. 10 Simplified models of possible interactions between NPs (*brown spheres*), alginates (*strands*) and cations (*small purple spheres*). **a** Alginates form bridges between NPs; **b** Each alginate strand envelopes one NP; **c** Alginates are partly crosslinked by cations forming ionic gels. This restricts the parts of the polymer available for binding NPs, and bridging can happen.
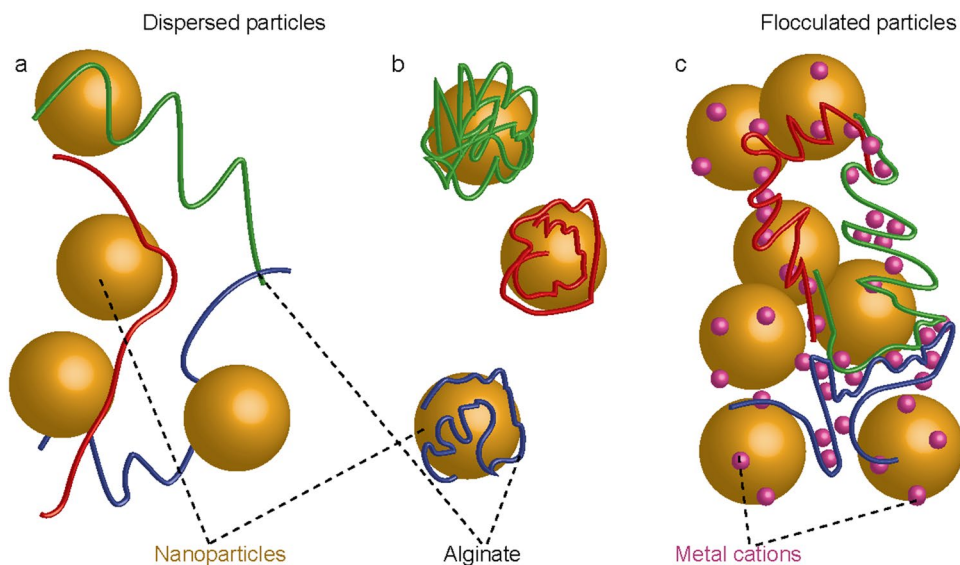
explained by assuming a flat conformation of the adsorbed polymer (Fig. 10b) [35, 51].

If this was the case, then the solution would be to attenuate the binding between the polymer and the NPs, and we tested the use of Ca^{2+} and Ce^{3+} cations for this purpose. It is well known that two G-blocks can crosslink via chelation of Ca^{2+} (Fig. 1), this is the basis for many of the applications of alginate hydrogels [15]. Formation of such junctions start with the exchange of the monovalent counterion attached to the carboxyl groups, in our case Na^+, with divalent or trivalent cations. Binding of cations to the alginate and formation of cross-linking junctions, will diminish the parts of the alginates available for binding to the NPs, and allow the alginate molecules to form bridges between the particles. Cations bound to the particles might participate in the bridging event. Alternatively, the NPs might become entangled in the formed gels. These options are not mutually exclusive and are depicted in Fig. 10c.

In our experiments we clearly see flocculation of both cerium and iron oxide NPs by LF 10/60 in the presence of Ca^{2+} (Fig. 5 and 6a, c), while the bacterial alginates do not seem to make aggregates. These alginates contain no G-blocks, and while Ca^{2+} bind G-blocks well, the binding of MG-blocks are much weaker and no binding to M-blocks is observed [52]. This would explain the absence of flocculation in the systems PfAc and PfdeAc with Ca^{2+}. These data strongly suggest that the formation of a gel network is a necessary factor in the observed flocculation of NPs using Ca^{2+} and G-block-containing alginate [25].

Trivalent cations have been found to crosslink alginate chains by binding to three carboxyl and hydroxyl groups [22, 24, 25], and their selectivity for specific block structures are much less [21] indicating that they are able to crosslink MG blocks or even M-blocks. When we replaced the divalent Ca^{2+} with Ce^{3+}, all three alginates made flocs in the presence of NPs and Ce^{3+}, again indicating that alginate cross-linking is necessary for flocculation. The C-2 oxygen has been implicated in hydrogen binding to trivalent cations [24], explaining why the O-2-acetylated alginate resulted in less flocs. A gel network was also seen by others when studying a mixture of alginate-coated hematite NPs and Ca^{2+} [29].

5 Conclusion

Our study shows that alginates can be used for flocculation of NPs if a suitable cation is present to cross-link the alginate molecules. The efficiency of flocculation is dependent on alginate composition and on the cation used to cross-link alginate molecules. In addition, acetylation of alginate strongly affects size and geometry of the flocks.

As described above, flocculation is used in various industries including the mineral processing industry. To develop alginate for this application, one needs to understand flocculation mechanisms and flocculant behavior in various systems, and a wider range of NPs, cations and characterized alginates should be studied and compared using the methods described in this study. Such studies should also include exploring the possibilities for selective flocculation of different NPs or minerals.

References

1. Obotey Ezugbe E and Rathilal S, *Membranes*, **10** (2020), https://doi.org/10.3390/membranes10050089.
2. Bratby J, *Coagulation and Flocculation in Water and Wastewater Treatment—Third Edition*, IWA Publishing, (2016), https://doi.org/10.2166/9781780407500.
3. Pearse M J, *Miner Eng*, **18** (2005) 139–149, https://doi.org/10.1016/j.mineng.2004.09.015.
4. King D J and Noss R R, *Rev Environ Health*, 8 (1989), https://doi.org/10.1515/reveh-1989-1-403.
5. Wang D, Liu X, Zeng G, Zhao J and Yang Q, *Water Res*, **130** (2018) 281–290, https://doi.org/10.1016/j.watres.2017.12.007.
6. Félix LL, Moreira GF, Filho LSL and Stavale F, *Miner Eng*, **178** (2022), https://doi.org/10.1016/j.mineng.2022.107429.
7. Matusiak J, Grządka E and Bastrzyk A, *Chem Eng J*, **423** (2021), https://doi.org/10.1016/j.cej.2021.130264.
8. Tian Z, Zhang L, Sang X, Shi G and Ni C, *J Phys Chem Solids*, **141** (2020) https://doi.org/10.1016/j.jpcs.2020.109408.
9. Sun Y, Shah KJ, Sun W and Zheng H, *Sep Purif Technol*, **215** (2019) 208, https://doi.org/10.1016/j.seppur.2019.01.017.
10. Mierczynska-Vasilev A, Kor M, Addai-Mensah J and Beattie D A, *Chem Eng J*, **220** (2013) 375, https://doi.org/10.1016/j.cej.2012.12.080.
11. Ertesvåg H, *Front Microbiol.* **6** (2015) 523. https://doi.org/10.3389/fmicb.2015.00523
12. Onsøyen E, *Carbohydr Europe* **14** (1996) 26.

13. Skjåk-Bræk G, Donati I, and Paoletti S, in *Matricardi P*, (eds) Alhaique F, and Coviello T, Characterization and Biomedical Applications, Pan Stanford Publishing Pte Ltd, Polysaccharide Hydrogels (2016), p 449.

14. Grand View Research, Alginate Market Size, Share and Trends Analysis Report By Type (High M, High G), By Product (Sodium, Propylene Glycol), By Application (Pharmaceutical, Industrial), By Region, And Segment Forecasts, 2021−2028, (2021), https://www.grandviewresearch.com/industry-analysis/alginate-market#, Accessed March 8th 2023

15. Nordgård C T and Draget K I, Chapter 26—Alginates, in: Phillips GO, Williams PA (Eds.) Handbook of Hydrocolloids (Third Edition), Woodhead Publishing (2021), pp. 805, https://doi.org/10.1016/B978-0-12-820104-6.00007-3.

16. Haug A and Larsen B, Biosynthesis of alginate. Epimerisation of D-mannuronic to L-guluronic acid residues in the polymer chain, *Biochim Biophys Acta*, 192 (1969) 557

17. Skjåk-Bræk G, Grasdalen H, and Larsen B, *Carbohydr. Res.* **154** (1986) 239.

18. Kloareg B, Badis Y, Cock J M and Michel G, *Genes (Basel)*, **12** (2021), https://doi.org/10.3390/genes12071059.

19. Aarstad O, Strand B L, Klepp-Andersen L M and Skjåk-Bræk G, *Biomacromol*, **14** (2013) 3409, https://doi.org/10.1021/bm400658k.

20. Smidsrød O, and Haug A, *Acta Chem Scand* **22** (1968) 1989.

21. Lunde G, Smidsrød O and Haug A, *Acta Chem Scand*, **26** (1972) 3421, https://doi.org/10.3891/acta.chem.scand.26-3421.

22. Massana Roquero D, Othman A, Melman A and Katz E, *Materi Adv*, **3** (2022) 1849, https://doi.org/10.1039/D1MA00959A.

23. Agulhon P, Markova V, Robitzer M, Quignard F and Mineva T, *Biomacromol*, **13** (2012) 1899, https://doi.org/10.1021/bm300420z.

24. Menakbi C, Quignard F and Mineva T, *J Phys Chemi B*, **120** (2016) 3615, https://doi.org/10.1021/acs.jpcb.6b00472.

25. Brus J, Urbanova M, Czernek J, Pavelkova M and Kulich P, *Biomacromol*, **18** (2017) 2478, https://doi.org/10.1021/acs.biomac.7b00627.

26. Maruyama H, Seki H and Igi A, *Biochem Eng J*, **162** (2020), https://doi.org/10.1016/j.bej.2020.107713.

27. Tripathy T, Karmakar N C and Singh R P, Development of novel polymeric flocculant based on grafted sodium alginate for the treatment of coal mine wastewater, *J Appl Pol Sci*, **82** (2001) 375, https://doi.org/10.1002/app.1861.

28. Liu C, Gao B, Wang S, Guo K and Xu X, *Carbohydr Polym*, **248** (2020), https://doi.org/10.1016/j.carbpol.2020.116790.

29. Chen KL, Mylon S E and Elimelech M, *Environ Sci Technol*, **40** (2006) 1516, https://doi.org/10.1021/es0518068.

30. Tripathy T & Singh RP, *Eurn Polym J*, **36** (2000) 1471, https://doi.org/10.1016/s0014-3057(99)00201-3.

31. Rani P, Mishra S and Sen G, *Carbohydr Polym*, **91** (2013) 686, https://doi.org/10.1016/j.carbpol.2012.08.023.

32. Chen W, Feng Q M, Zhang G F, Yang Q and Zhang C, *Miner Eng*, **113** (2017) 1, https://doi.org/10.1016/j.mineng.2017.07.016.

33. Moral Ç K, Ertesvåg H and Sanin F D, *Environ Sci Pollut Res* (2016) 1, https://doi.org/10.1007/s11356-016-7475-6.

34. Fu Y F, Yin W Z, Yang B, Li C and Li D, *Int J Miner Metall*, **25** (2018) 1113, https://doi.org/10.1007/s12613-018-1662-z.

35. Vajihinejad V, Gumfekar S P, Bazoubandi B, Rostami Najafabadi Z and Soares J B P, *Macromol Mater Eng*, **304** (2019) 1800526, https://doi.org/10.1002/mame.201800526.

36. Greenwood NN & Earnshaw A, *Chemistry of the Elements*, 2 ed., Elsevier, (2012).

37. *Gimmestad M, Sletta H, Karunakaran K P, Bakkevig K, Ertesvåg H, Ellingsen T, Skjåk-Bræk G, Valla S, inventors; FMC Biopolymer AS assignee, New Mutant Strains of Pseudomonas Fluorescens and Variants Thereof, Methods of Their Production, and Uses Thereof in Alginate Production*. WO2004/011628, (2002).

38. Riddick T M and Zeta-Meter I, *Control of Colloid Stability Through Zeta Potential: With a Closing Chapter on Its Relationship to Cardiovascular Disease*, Zeta-Meter, Incorporated, (1968).

39. Pochapski D J, Carvalho Dos Santos C, Leite G W, Pulcinelli S H and Santilli C V, *Langmuir*, **37** (2021) 13379, https://doi.org/10.1021/acs.langmuir.1c02056.

40. Zhang Y, Chen Y, Westerhoff P, Hristovski K and Crittenden J C, *Water Res*, **42** (2008) 2204, https://doi.org/10.1016/j.watres.2007.11.036.

41. He Y T, Wan J and Tokunaga T, *J Nanopart Res*, **10** (2007) 321, https://doi.org/10.1007/s11051-007-9255-1.

42. Baalousha M, Ju-Nam Y, Cole P A, Hriljac J A and Lead J R, *Environ Toxicol Chem*, **31** (2012) 994, https://doi.org/10.1002/etc.1786.

43. Shchukin E D A V P, Amelina E A, and Zelenev AS, *Colloid and Surface Chemistry*, Elsevier Science, (2001).

44. Pietroiusti A, Stockmann-Juvala H, Lucaroni F and Savolainen K, *WIREs NanomedNanobiotechnol*, **10** (2018), https://doi.org/10.1002/wnan.1513.

45. Wigginton N S, Haus K L and Hochella Jr M F, *J Environ Monit*, **9** (2007), https://doi.org/10.1039/b712709j.

46. Piccinno F, Gottschalk F, Seeger S and Nowack B, *J Nanopart Res*, **14** (2012), https://doi.org/10.1007/s11051-012-1109-9.

47. Mohapatra D P and Kirpalani D M, *Nanotechnol Environ Eng*, **2** (2016), https://doi.org/10.1007/s41204-016-0011-6.

48. Almeida V O D, Pereira T C B, Teodoro L D S, Escobar M and Schneider I A H, *Sci Total Environ*, **759** (2021), https://doi.org/10.1016/j.scitotenv.2020.143456.

49. Cosgrove T, *Colloid Science: Principles, Methods and Applications*, John Wiley & Sons, (2010).

50. Ostolska I and Wiśniewska M, *Colloid Polym Sci*, **292** (2014) 2453, https://doi.org/10.1007/s00396-014-3276-y.

51. Gregory J, *Colloids Surf*, **31** (1988) 231, https://doi.org/10.1016/0166-6622(88)80196-3.

52. Mørch Ý A, Donati I, Strand B L and Skjåk-Bræk G, *Biomacromol*, **7** (2006) 1471, https://doi.org/10.1021/bm060010d.